PIV MEASUREMENT OF TURBULENT JET AND POOL MIXING PRODUCED BY A STEAM JET IN A SUBCOOLED WATER POOL

Yeon Jun CHOO, Chul Hwa SONG* and Young Jung YOUN

Korea-Atomic Energy Research Institute
Daeduk-daero 1045, Yuseong-gu Daejeon, 305-353, Republic of Korea
**Corresponding Author: chsong@kaeri.re.kr*

Abstract

This experimental research is on the fluid-dynamic features produced by a steam injection into a subcooled water pool. The relevant phenomena could often be encountered in a water cooled nuclear reactor. Two major topics, the turbulent jet and internal circulation produced by a steam injection, were investigated separately using a particle image velocimetry (PIV) as a non-intrusive optical measurement technique. The results of the turbulent jet experiments (under the unconfined and upward discharging conditions) provided the parametric values quantitatively for describing a turbulent jet such as the self-similar velocity profile, central velocity decay, spreading rate, etc. On the other hand, for the internal circulation (under the confined and downward discharging conditions) produced by a steam injection, the typical flow patterns of the whole pool region were measured and these results show some useful information. Physical domains of both experiments have a 2-D axially symmetry geometry and the boundary and initial conditions which can be readily and well defined. Moreover, the quantitative data of this research would be used as benchmarking data for a CFD simulation of the relevant phenomena.

1. INTRODUCTION

Direct Contact Condensation (DCC) may be regarded as an inevitable phenomenon in a water cooled nuclear reactor. In the design of the APR 1400, the In-containment Refueling Water Storage Tank (IRWST) is equipped to take precautions against an emergent accident, such as a Loss of Coolant Accident (LOCA). A large amount of steam generated during these accidents is blown down into the subcooled water in the IRWST. At this time, a very effective heat and mass transfer through the DCC between the hot steam and the subcooled water occurs. Many large and small scale experiments to investigate the thermo-hydraulic characteristics in this circumstance have been conducted (Weimer, 1973, Kim, 1997 and Cho, 1998). Most studies have, however, focused on a steam jet oscillation, shape, length and condensational heat transfer. In addition, these experimental researches have only been interested in the steam plume characteristics.

General characteristics of free shear single phase jets are already explained well in many textbooks(Pope, 2000) and open literatures. However, a lack of studies about the steam-induced turbulent jet flow exists. The turbulent jet produced by a steam injection is an important topic because the effectiveness of a thermal mixing in a pool and the safety concerns of circumferential structures are dominated by the overall features of this steam-induced turbulent jet. Kim and Youn(2008) measured the velocity distribution of a condensed turbulent jet by a single hole sparger using a point-wise Pitot tube and compared the measured velocity profiles with theoretical models. Even though their results have provided the information about the mixing characteristics of a steam injection, they were, however, limited to a local measuring technique. Wissen et al. (2005) firstly measured the characteristics of a turbulent jet from a ring-shaped orifice using PIV and presented a detailed comparative dataset. However, their results are valid only for their specific type of orifice. On the other hand, few researchers (Kang, 2007, Gamble, 2001) have tried to simulate the overall pool mixing phenomena using computational fluid dynamics (CFD). CFD has been a useful tool in a practical sense in many industrial field as well as nuclear engineering. Simultaneously, CFD analysis contends with different types of errors (e.g. numerical, model, user and etc) so that an verification with a credible experimental value is strongly recommended to ensure a correct implementation of all numerical and physical models in the CFD method. Nevertheless, it is a fact that there is a lack of

proper experimental data for a steam-induced turbulent jet or pool mixing phenomena.
The present experimental study will deal with two major topics: the turbulent jet and the pool mixing produced by a steam injection, and introduce a benchmarking data set for a numerical simulation of the relevant problems.

2. EXPERIMENTAL FACILITY

The experimental facility, JICO (abbreviation of Jet Injection and Condensation), used in this research is shown in Fig. 1. The JICO was designed as a simple and multipurpose facility, in which the various jets and pool mixing phenomena, e.g. condensing jet, single or two phase jet, plunging jet and pool mixing driven by jet, can be realized. All directions are optically accessible through transparent windows (acrylic material), so that non-intrusive optical measurement techniques such as PIV LDV, etc. as well as a visualization can be applicable in principal. Moreover, alternative choice of an upward or downward injection of a jet and a replaceability of a nozzle allow for various tests to be performed.
Three main parts of the JICO are the test section, the steam generator and the measurement unit (PIV). The PIV measurement system will be explained later in Section 4 and the remaining parts are as follows. Test section is divided into 1) an inner cylinder (an inner diameter of 0.78 m and a height of 2 m) as a real interest domain and 2) an outer square tank (a square cross section of 1 m × 1m and a height of 1.8 m) as an auxiliary part 3) injection nozzle. Two overflow lines (ø = 50 mm) maintain constantly the water level in the inner cylinder by a height of 1825 mm roughly. The outer square tank has two functions to eliminate an optical distortion and to minimize a heat loss through the cylinder wall. Three thermocouples are installed into the inner cylinder wall to measure the temperature of the pool water. Maximum operating pressure and temperature of the test section are an ambient pressure and 70 ^{o}C. Steam generator has a maximum steam generation rate of 0.023 kg/sec, a maximum operating pressure of 10 kPa and a feeding system for a continuous operation. Water storage tank has a capacity of about 0.5 m^3 and an immersion electrical heater of 12 kW. Before the water in the storage tank is fed into the steam generator, it is pre-heated for the sake of a degassing.
In the case of the turbulent jet experiment, the steam nozzle is installed at the bottom plate with an upward-facing direction. On the other hand, in the pool mixing experiment, one is held with fore arms in the air with a downward-facing direction respectively. The detailed dimensions and shape of a nozzle are shown in Fig. 2. In order to avoid a complex geometry of a nozzle shape, the steam nozzle has a single hole with a sharp edge and a straight flow channel. In order to minimize the pressure drop and to develop a velocity profile completely at a nozzle exit, a gradually-converged type of a nozzle flow channel is adopted. In addition, the insulation tube enveloped on the nozzle outside surface makes it possible to minimize the heat loss though the submerged part of the steam nozzle. Steam temperature and pressure are measured at the inlet part of the nozzle.

3. DISCRIPTION OF PROBLMES

3.1 Turbulent jet

From a practical viewpoint of the V&V of a CFD, it is a matter of course that the measured results for a simple domain are more proper. The present subject is, therefore, on the assumption of a 2D-axisymmetric one as a spatial domain and a steady-state one as a dynamic equilibrium. Figure 3(a) shows the schematic description of the geometrical conditions of the target domain in the case of the turbulent jet experiment. The nozzle is installed vertically at the bottom so that the jet axis collapses with the axisymmetric line of the target domain. As a matter of convenience, a wall condition can be assumed as an adiabatic condition; the actual heat loss through the wall and water surface is negligible during the test.
Water surface is constantly maintained at a 1825 mm height by an overflow hole. The radial width from the jet axis to the wall boundary is 390 mm, i.e. the ratio of the radial distance from the nozzle center to the wall to nozzle exit diameter (D/d) is 156, so that we can assume an unconfined condition. The initial velocity profile at the nozzle exit can be regarded as a fully developed condition because of the straightly elongated flow channel (L/d = 20).
Since the supplied steam mass flux is small compared with the total amount of the pool water and the strength of the current through the overflow hole is weak, therefore, the influence of the free surface

on the nature of the turbulent jet itself can be ignored. Test matrix for the turbulent jet experiments is shown in Table 1.

3.2 Pool mixing

During the blowdown period of a LOCA, steam or high-energy liquid is discharged into the suppression pool and a strong thermo-hydraulic mixing process is consequently generated in the pool. In a real suppression pool, the radial injection direction and the multi-hole sparger make the flow nature asymmetric and transient; it means that it's difficult to simulate and measure a real situation. Moreover, even if it is possible, the real complex situation would increase the uncertainty of the measurement results as well as the numerical simulation. For these reasons, pool mixing experiments were carried out with simple cases for the turbulent jet experiments. Differences for the turbulent jet experiment are the jet injection direction and the free surface level. A vertical-downward injection when compared with upward one is more advantageous for inducing a strong internal circulating flow just like the impinging jet. The level of the free surface is 850 mm in height and the steam nozzle is immersed at about 60 mm in depth. From a visual observation in this condition, the free surface is still at this height. Test matrix for the pool mixing experiments is also shown in Table 1.

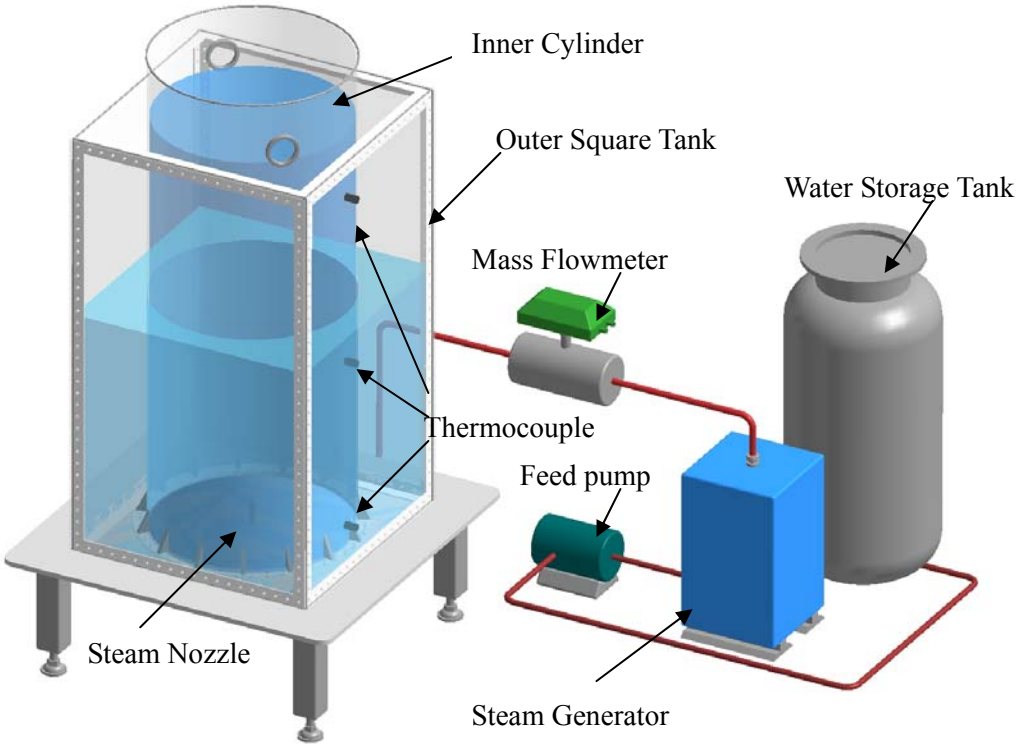

Fig 1: JICO experimental facility

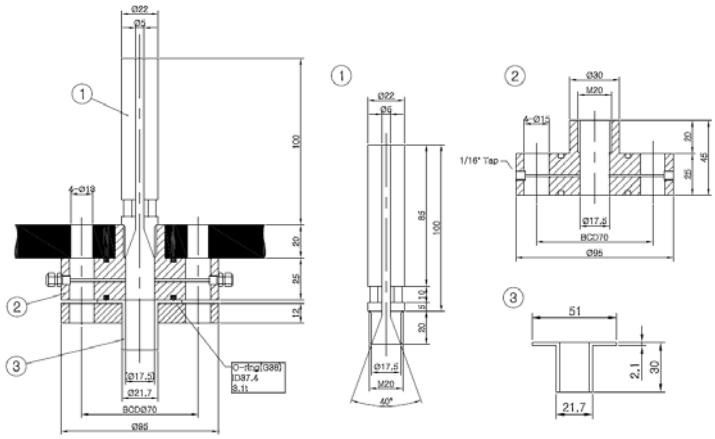

Fig 2: Steam nozzle (all unit is in millimeter).

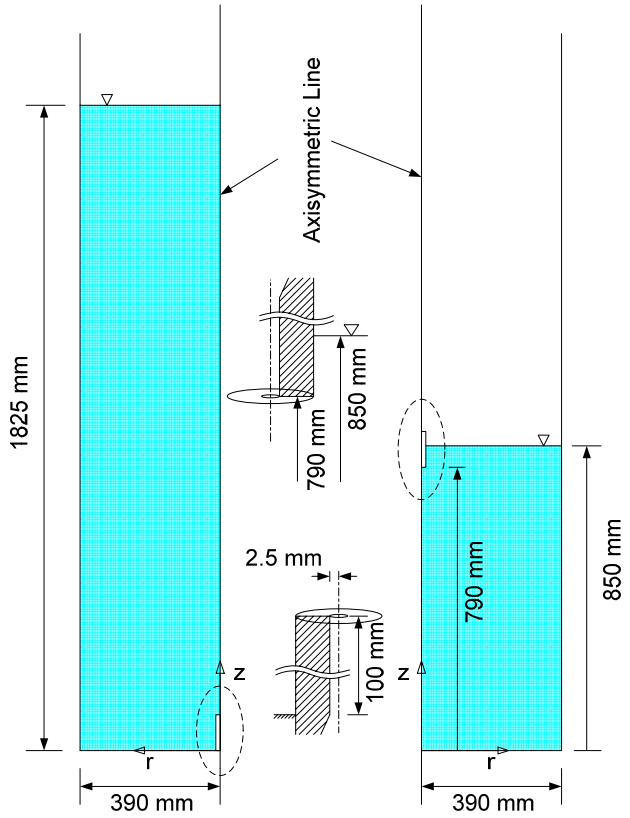

Fig 3: Geometrical description of the experiment (turbulent jet and pool mixing)

Table 1: Test Matrix for the turbulent jet and pool mixing experiments

Experiments	Test I.D.	Mass flux Kg/m^2s	Steam Temp. ^oC	Nozzle Pres. kPa	Pool Temp. ^oC
Turbulent Steam Jet	M300T30	300.28	137.64	205.67	30.09
	M300T60	300.06	137.52	204.13	60.01
	M450T30	450.89	151.92	356.66	30.10
	M450T40	450.72	151.96	356.60	40.14
	M450T50	450.05	151.96	357.32	50.14
	M450T60	451.45	151.85	356.80	59.97
	M650T30	648.39	166.98	574.56	30.33
	M650T30	647.42	166.75	572.02	60.04
Pool Mixing	M300T45	300.81	135.95	204.12	45.10
	M450T45	449.22	151.88	357.20	45.67
	M650T45	650.77	165.12	571.86	44.96

3. MEASUREMENT TECHNIQUE AND UNCERTAINTY ANALYSIS

3.1 PIV technique

In the present research, PIV technique is used to measure the velocity filed of a turbulent jet and a pool mixing driven by a steam injection. In recent years, the PIV measurement technique has shown promise in fluid flow researches and has been used very extensively for velocity field measurements in particular due to its a non-intrusive capability. A typical PIV system comprised of two systems i.e. image capture and image analysis, was used. In the image capture system, the light source is a double-head Nd-YAG laser (Continuum) operated at a frequency of 10 Hz and a power of 200 mJ per pulse at λ=532 nm. MegaPlus ES1.0 PIV camera (1018 × 1008 pixels) operated in a triggered double exposure

mode is coupled with 60 mm Nikon microlens. With this system, two paired-instantaneous particle images are stored in a synchronized PIV processor (PIV 2100, Dantec Inc.) and transferred to a PC. Small non-condensable bubbles (10~100 μm) could be incidentally used as tracer particles. In the condensation process of a steam plume, the production of non-condensable gas bubbles is almost unavoidable. Nevertheless, it was judged that these bubbles are enough to follow a jet flow with a high momentum. However, since local zones could exist where even the small bubbles can't represent the liquid phase current, this non-condensable gas bubble couldn't be used as a tracer in the pool mixing experiment. Therefore, fluorescent solid tracer particles (Dantec Inc. FPP-RhB-35, 20~50 μm) are dispersed into the pool in the pool mixing experiment, contrary to the turbulent jet experiment. The signals scatted from fluorescent particles can be imaged through a narrow band pass filter attached to a lens.

In the stage of an image analysis, Adoptive Cross Correlation (ACC) would be a more useful algorithm in the case of measuring the velocity for the free shear layer, in which a larger velocity gradient inside an observation area can exist and introduce the possibility of an erroneous calculation and/or under-estimation. For this reason, two steps of an ACC are adopted in this research. The initial interrogation widow is 64 × 64 pixels and then the refinement process is conducted at 32 × 32 pixels over 2 steps.

The measuring strategies of both experiments are shown schematically in Figure 4. The measuring field of view of the PIV camera in the turbulent jet and pool mixing experiments are 100 × 100 mm and 400 × 400 mm respectively. In the turbulent jet experiment, one camera scans the target area along axial direction of the jet from the nozzle exit to far downstream (z/d ≈ 0 to 100) over 6 intervals. In the pool mixing experiment, two horizontally-mounted cameras simultaneously capture the particles image of the whole test section.

In the region of the steam plume and the dense non-condensable gases at the near field of the nozzle exit (over 70~90 mm from the nozzle exit), i.e. at the lower right part of region 1 in Figure 4(a) and the upper left part in Figure 4(b), a measurement of the velocity is difficult and if possible the result would be unreliable. Figure 5 shows the typical images captured in both experiments. As shown in the image of region 1, a separated particle's signal cannot be observed. Along the downstream, the moderate density of the bubble scattering allows for an efficient vector calculation. In the case of the pool mixing experiment, two cameras cover the entire internal region of the test section as shown in Figure 5 (b).

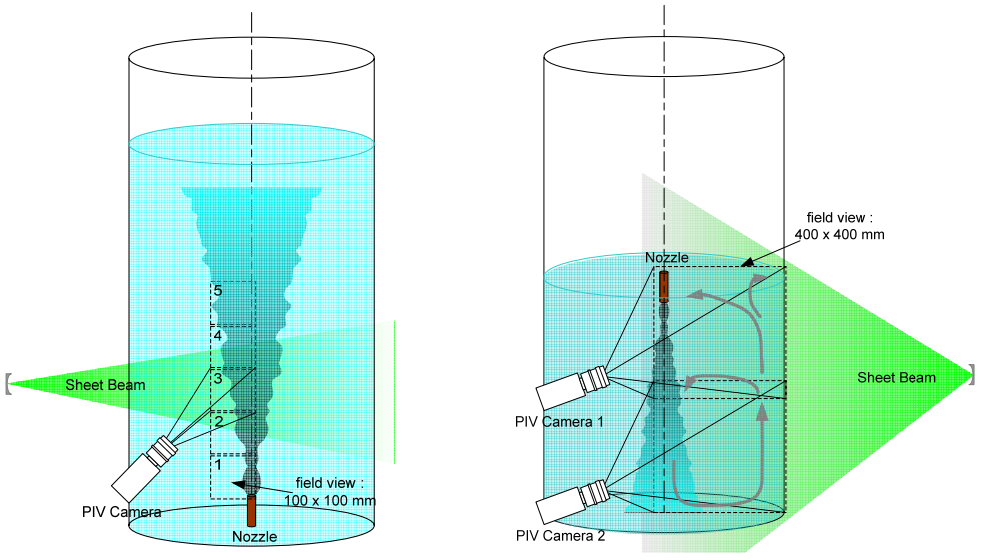

(a) Turbulent jet experiment (b) Pool mixing experiment

Fig 4: Schematic representation of the PIV measurement

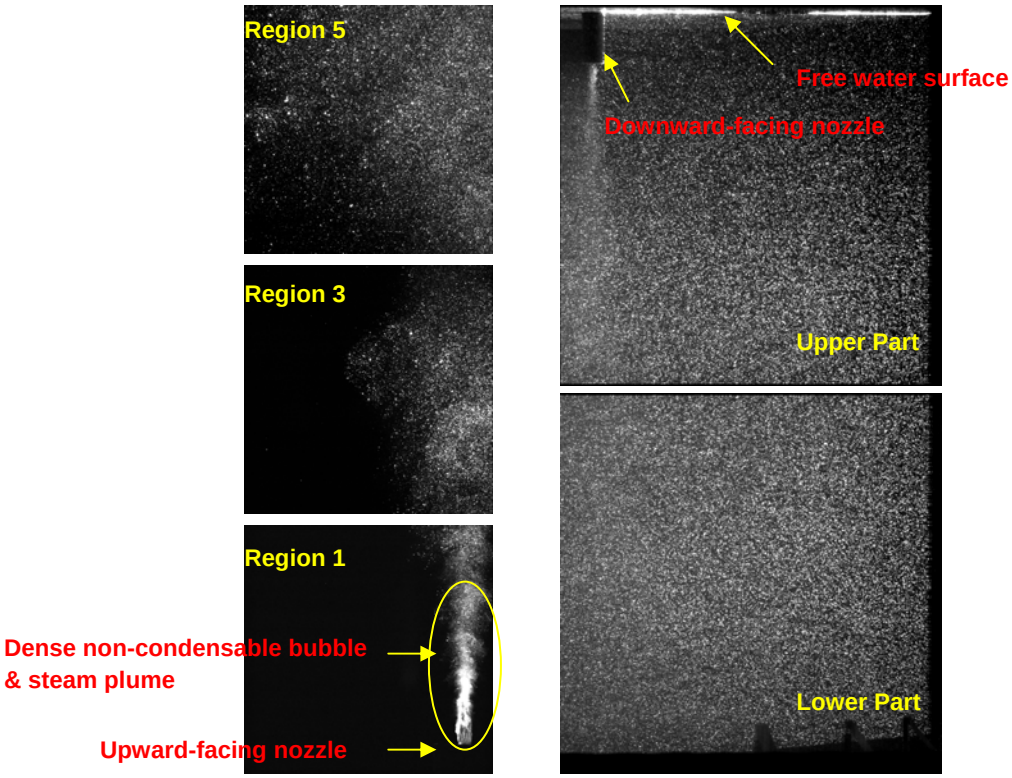

a) Turbulent jet experiment b) Pool mixing experiment

Fig 5: Typical PIV images

3.2 Error analysis

Uncertainties of the velocity measurement and experimental parameters are presented below according to the ISO GUM Guide.

Temperature

Three K-type thermocouples and one K-type thermocouple (WATLOW Inc.) are employed for the pool temperature at three vertical places and the steam temperature at the nozzle exit respectively. Type B uncertainties of each error source are estimated as follows; K-type thermocouple: 0.8 ^{o}C, compensation cable: 1.1 ^{o}C and DMM: 1.0 ^{o}C. An extended uncertainty of the temperature was ±1.910 ^{o}C in 95 % confidence level (k-factor 1.96).

Mass Flux

Steam mass flux injected by a nozzle is measured by a Vortex-type mass flowmeter (OVAL, EX DELTA) which has an accuracy of ±1% of a reading value. Including the uncertainties of the DMM (0.0035% of a reading and 0.0005 % of a span) and the voltage converter (0.1 % of reading), an extended uncertainty of the steam mass flux was ±3.196 kg/m^{2}s at a 95 % confidence level (k-factor 1.96).

Pressure

Uncertainty of the nozzle exit pressure measured by the pressure senor (Rosemount 3051S, 0.15 % of span) was estimated as ±3.127 kPa at a 95 % confidence level (k-factor 1.96).

Velocity by tthe PIV technique

The bias error of the instantaneous velocity vector measured by the PIV technique is combined with two major errors due to the timing interval and the peak displacement detected during the correlation calculation. Typically, a FFT based correlation algorithm has an accuracy from about 0.25 to 0.1 pixels.

While on the other, the time interval error can be considered to be negligible. Another source of an uncertainty that can occur in an experiment is one induced by distorted images which result from a local temperature gradient, that is, a non-uniform refractive index. Such an undesirable effect is, however, not so dominant. Temperature of the steam condensate decreases rapidly due to a thermal mixing with a high subcooled water. Actually, except for directly downstream of the steam nozzle, the maximum temperature difference is within a few degrees, so that this effect on the uncertainty could be insignificant. Consequently the uncertainty of the instantaneous velocity is conservatively 1 % of an absolute value with a consideration of the other uncertainty elements such as the scaling factor between the image and real dimensions, an optical distortion of the observation window, etc. Finally, if an additional random error by averaging the instantaneous velocities (300~800 samples) is considered together with two sigma (2σ), the total uncertainty of the velocity could be approximately 1.7 % ~ 2.5 % of an absolute value.

4. RESULT AND DISCUSSION

As mentioned before, the present experimental study was carried out on the hydraulic characteristics of a turbulent jet and a pool mixing driven by a steam injection. The results of these two topics (Section 4.1: Turbulent jet driven by steam injection and Section 4.2: Internal circulation in a confined pool) will be discussed in this section.

4.1 Turbulent jet driven by steam injection

Analytical and experimental approaches for the mean quantities of free shear flows have been established comparatively well as far as a single phase jet, i.e. air to air and liquid to liquid is considered. Unlike the single phase jet, it is true that further researches on a steam-driven turbulent jet with a condensation process, as in this research, is required. Therefore, it is expected that the results described in this section could be used in the related researches, as well as in the validation of a CFD simulation.

4.1.1 The instantaneous and mean velocity field

The typical instantaneous velocity vectors and magnitude contours between z/d = 36 and 55, i.e. in region 2 in Fig. 4(a), are presented in Fig. 6(a). The inherent oscillating manner of the jet is clearly shown, reflecting the feature of an entrainment of the jet and its interaction with the ambient water. Evidently as well, the highest velocity contours occur in the central region. On the other hand, the mean velocity (Fig. 6(b)) shows clear profiles. In practice, some physical assumptions as for a free shear layer (jet, wake and simple shear layer) allow for the turbulent flow to be transformed into a mathematically analyzable form. Also in the steam-driven turbulent jet, the theoretical description of the mean flow characteristics of the single phase turbulent jet can be compatible. Consequently the mean flow features of the turbulent jet are regarded as a useful tool for characterizing a turbulent jet. Based on it, our experimental results will be analyzed and adjusted.
Fig. 7 shows the entire vector filed which is measured and integrated by means of scanning the target region over 6 intervals. This is, in appearance, similar as the single phase turbulent jet. Actual measured region is to z/d = 100 in all cases of the turbulent jets experiment. It is clearly observed that the central velocities are decayed due to the turbulent dissipation and the velocity profiles are spread to the extent of rate at which the shear layer grows laterally with the axial distance.

4.1.2 Self-similarity

The concept of a self-similarity (or self-preservation) implies that the flow has reached a dynamic equilibrium or asymptotic state in which the mean and higher-order moments evolve together (Townsend 1976). Typically, self-similar quantities are represented by scaled dependent variables and show a universal aspect over a fully developed region. Two general characteristic scales are the mean centerline maximum velocity, $U_C(z)=U(z,0)$, and a jet's half width $r_{1/2}$ in a round shear jet. In addition, since a jet's half width is dependent on $(z-z_0)$, $r/(z-z_0)$ can be an alternate cross-stream scale. Consequently the cross-stream similarity variable can be taken to be either

$$\xi = \frac{r}{r_{1/2}} \quad \text{or} \quad \eta = \frac{r}{z - z_0}$$

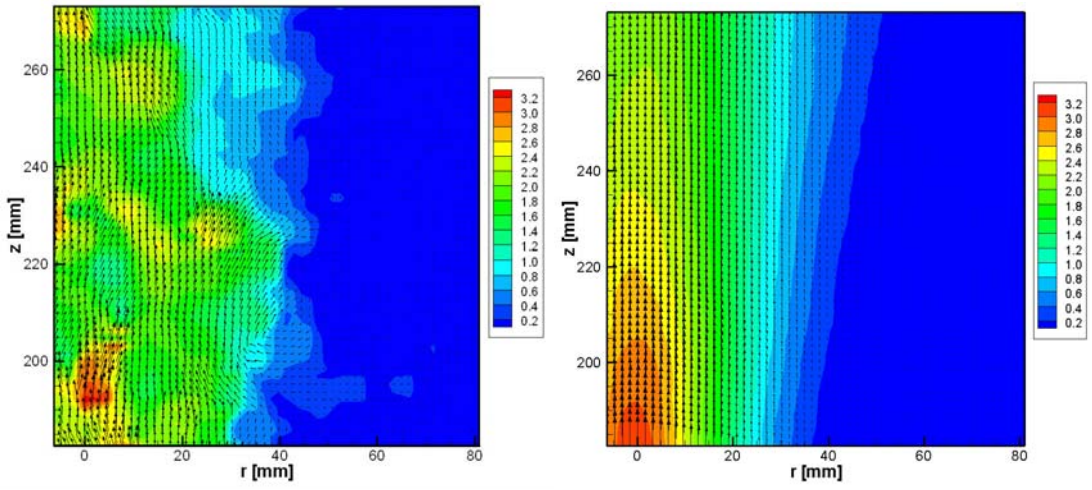

(a) (b)

Fig 6: Typical instantaneous and averaged velocity vectors and contours of their magnitudes

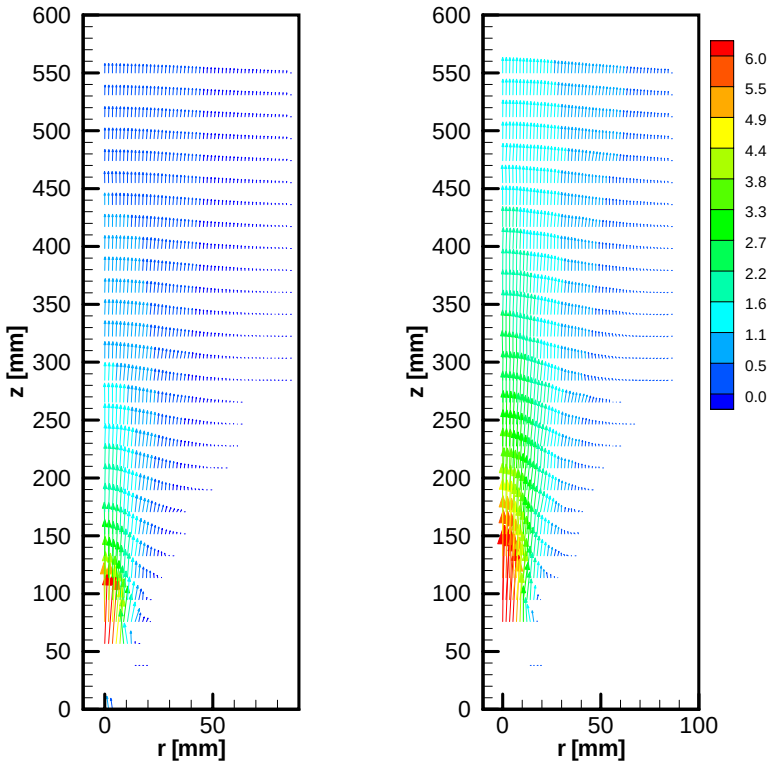

(a) (b)

Fig 7: Overall velocity pattern of M300T60 and M650T60

Here, z_0 is the virtual origin. Measurements of single-phase jets indicate that in the far field centerline velocity U_C is inversely proportional to the distance:

$$U_C = \frac{C}{z - z_0}$$

with C a coefficient determined by an experimental value. Since a jet's momentum induced by steam injection can affect the safety of submerged structures, the central line velocity decay rate is a key feature of the steam-induced turbulent jet. Fig. 8 shows the development of the mean center-line velocity as a function of the distance from the nozzle. From these result, a coefficient C and virtual origin z_0 can be determined. Next the mean axial velocity normalized by the centerline velocity, U/U_C

is plotted versus the dimensionless radial coordinate, η in Fig. 9. Generally, a Gaussian profile can be fitted accurately with experimental data;

$$\frac{U}{U_C} = \exp(-K\eta^2)$$

The collapse of all the measurements for the single fitting profile reflects that a jet has a good self-similar feature. Another coefficient of the spreading rate, *S*, is defined as follows;

$$S = \frac{r_{1/2}(z)}{(z - z_0)}$$

All the fitted coefficients mentioned above are summarized in Table 2. The coefficient *C* is strongly dependant on the mass flux, i.e. it increases with the mass flux. In contrast to most previous results in the literature on single phase/non-condensing jets, the virtual origin z_0 for this condensing jet is always negative. Actually, the steam plume near the exit of the nozzle has a particular shape, differing from a single phase jet, and a strong driving force and phase change of the steam could influence the near field condition of the jet. The difference in the virtual origin from a single phase jet results from the inherent nature of the steam-driven turbulent jet. Almost the same spreading rates as a single phase/non-condensing jet, about 0.097, were found to be between 0.090~ 0.098. It means that the spreading rate exhibits the tendency of the a dependency on the source of a momentum. These results are consistent with those by Wissen et al (2005).

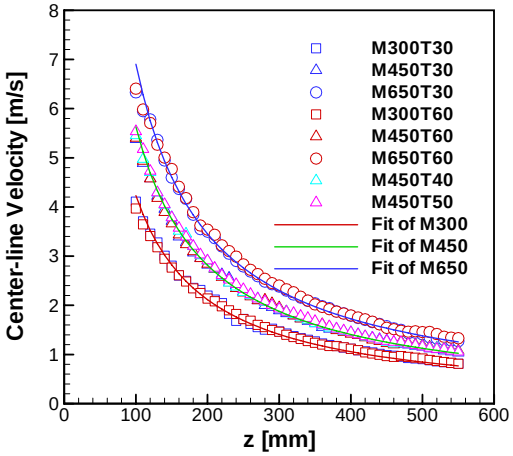

Fig. 8: The centerline velocity as a function of the distance to the steam nozzle

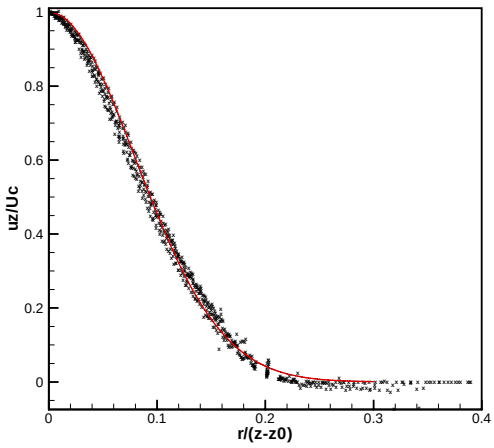

Fig. 9: The self-similar profile of the mean axial velocity in the

Table 2. Fitted coefficients of self-similar turbulent flow for all test matrix
(95% confidence interval within parentheses)

Test I.D.	C	z_0	K	S
M300T30	457.1 (446.3 ~ 467.8)	-13.10 (-18.630 ~ -7.571)	86.0157	0.0898
M300T60	460.2 (454.9 ~ 465.5)	-15.40 (-18.150 ~ -12.650)	84.4252	0.0906
M450T30	586.7 (578.2 ~ 595.3)	-8.535 (-11.890 ~ -5.179)	79.3095	0.0935
M450T40	580.8 (573.9 ~ 587.7)	-2.583 (-5.211 ~ 0.045)	82.8969	0.0914
M450T50	587.2 (583.1 ~ 591.4)	-3.768 (-5.348 ~ -2.188)	81.8818	0.0920
M450T60	596.5 (587.0 ~ 606.0)	-12.42 (-16.170 ~ -8.678)	72.3851	0.0979
M650T30	716.1 (706.6 ~ 725.6)	-5.075 (-8.075 ~ -2.093)	78.8375	0.0938
M650T60	720.1 (711.0 ~ 729.2)	-2.943 (-5.745 ~ -0.140)	74.9832	0.0961

4.2 Internal circulation driven by steam injection

Turbulent jet which was strongly induced by a steam injection entrains the surrounding water and creates an internal circulation pattern within a pool; it leads to a mixing of the pool contents. Fig. 8 demonstrates that a coherent circulating flow pattern is created by the steam injection. As expected, stronger internal driving flows can be observed with an increasing mass flux. Key feature of the internal flow pattern in the pool mixing is the location of the center of the recirculation and the existence of a secondary flow. For all the tests, the eye of a strong recirculation was placed at the bottom right-hand corner. With an increasing mass flux, the eye of the recirculation was moved upward by the relatively strong entrainment and a bouncing flow (Fig. 9). Moreover, an apparent secondary flow appeared for the result of a mass flux at 650 kg/m^{2}s. It is caused by the stronger bouncing flow along the right wall which tows the comparatively still water at the upper right region.

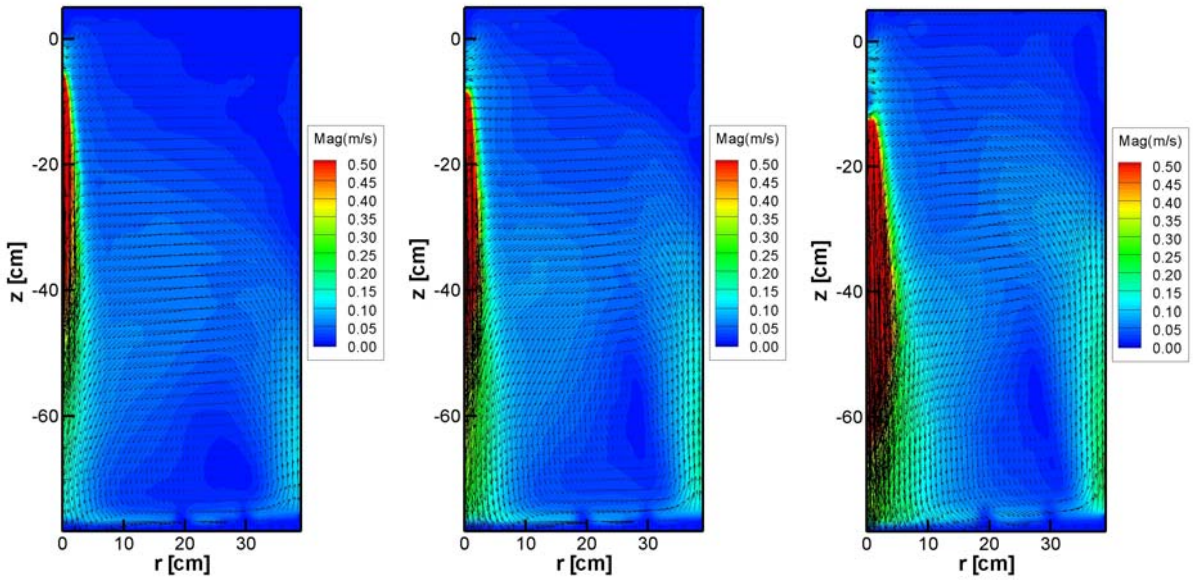

Fig. 8: Internal circulation pattern and velocity field for mass flux of 300, 450 and 650 kg/m^{2}s with a pool water temperature of 45 ^{o}C.

5. CONCLUSION

Experimental studies on a turbulent jet and a pool mixing pattern produced by a steam injection were conducted separately using the PIV measurement technique. Self-similar features of the turbulent jet within the axially symmetric test domain were measured in detail and the fitted coefficients are presented for all test matrices. Internal circulation pattern for the injected steam mass flux was measured over the whole test domain. The experiment results of both topics revealed the detailed

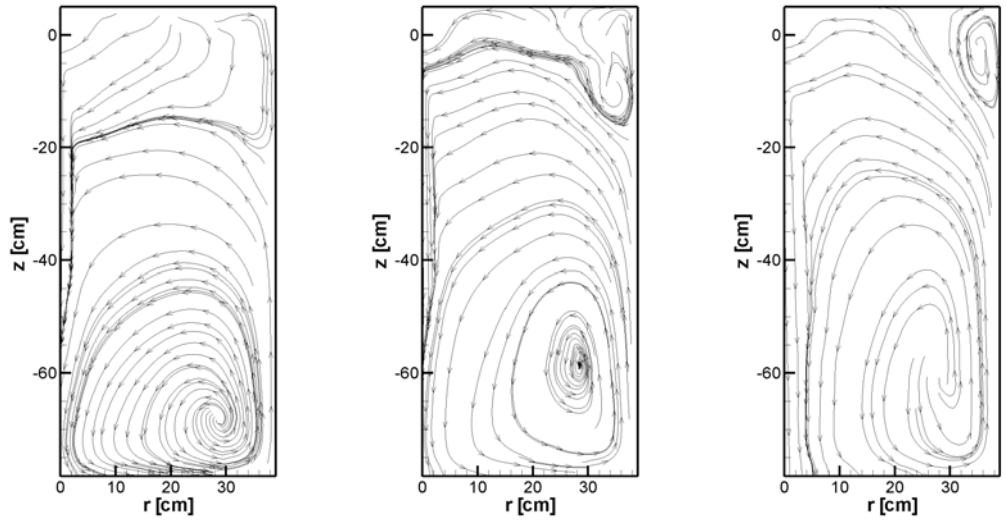

Fig. 9: Stream pattern for the same case of Fig. 8

velocity structures quantitatively and could be used as the benchmarking data for the validation of a CFD simulation of the relevant phenomena that appear in the nuclear reactor safety problems.

ACKNOLEDGEMENT

This work was financially supported for the Nuclear R&D Program from the Ministry of Science and Technology of Korea. The authors are sincerely gratefully for the financial support.

REFERENCES

H.S. Kang and C.H. Song, "CFD analysis for thermal mixing in a subcooled water tank under a high steam mass flux discharge condition", Nuclear Engineering and Design, Vol. 238, pp. 492-501 (2007).

J.C. Weimer, G.M. Feath and D.R. Olson, "Penetration of vapor jets submerged in subcooled liquids", AIChE Journal, Vol. 19, 552-558 (1973).

R.E. Gamble, et al., "Pressure suppression pool mixing in passive advanced BWR plants", Nuclear Engineering and Design, Vol. 204, pp. 321-336 (2001).

R.J.E. van Wissen, et al., "Particle image velocimetry measurements of a steam-driven confined turbulent water jet", J. Fluid Mech. Vol. 530, pp. 353-368 (2005).

S. Cho, et al., "Experimental study on dynamic pressure pulse in direct contact condensation of steam discharging into subcooled water", *The 1st Korea-Japan Symposium on Nuclear Thermal Hydraulics and Safety (NTHAS98)*, Pusan, Korea, pp. 291-298 (1998).

S.B. Pepe, "Turbulent Flows", Cambridge University Press, New York, 2000.

Y.S. Kim, et al., "An experimental investigation of direct condensation of steam jet in subcooled water", Journal of the Korea Nuclear Society, Vol. 29, pp. 45-57 (1997).

Y.S. Kim and Y.J. Youn, "Experimental study of turbulent jet induced by steam jet condensation through a hole in a water tank", International Communications in Heat and Mass Transfer, Vol. 35, pp. 21-29 (2008).